

# Influence of the Intermediate Density-of-States Occupancy on Open-Circuit Voltage of Bulk Heterojunction Solar Cells with Different Fullerene Acceptors

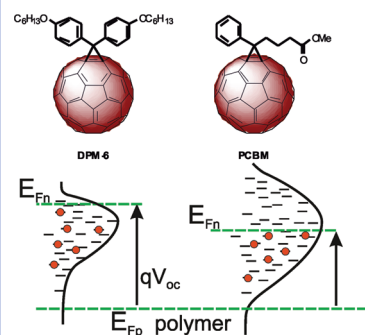
Germà Garcia-Belmonte,<sup>\*,†</sup> Pablo P. Boix,<sup>†</sup> Juan Bisquert,<sup>\*,†</sup> Martijn Lenes,<sup>‡</sup> Henk J. Bolink,<sup>‡</sup> Andrea La Rosa,<sup>§,||</sup> Salvatore Filippone,<sup>§,||</sup> and Nazario Martín<sup>§,||</sup>

<sup>†</sup>Photovoltaic and Optoelectronic Devices Group, Departament de Física, Universitat Jaume I, 12071 Castelló, Spain,

<sup>‡</sup>Instituto de Ciencia Molecular, Universidad de Valencia, P.O. Box 22085, 46071 Valencia, Spain, <sup>§</sup>Departamento de Química Orgánica, Facultad de Química, Universidad Complutense, 28040 Madrid, Spain, and <sup>||</sup>IMDEA-Nanociencia, 28049 Madrid, Spain

**ABSTRACT** Electron density of states (DOS) and recombination kinetics of bulk heterojunction solar cells consisting of a poly(3-hexylthiophene) (P3HT) donor and two fullerene acceptors, either [6,6]-phenyl-C<sub>61</sub>-butyric acid methyl ester (PCBM) or 4,4'-dihexyloxydiphenylmethano[60]fullerene (DPM<sub>6</sub>), have been determined by means of impedance spectroscopy. The observed difference of 125 mV in the output open-circuit voltage is attributed to significant differences of the occupancy of the DOS in both fullerenes. Whereas DPM<sub>6</sub> exhibits a full occupation of the electronic band, occupancy is restricted to the tail of the DOS in the case of PCBM-based devices, implying a higher rise of the Fermi level in the DPM<sub>6</sub> fullerene. Carrier lifetime describes a negative exponential dependence on the open-circuit voltage, exhibiting values on the microsecond scale at 1 sun illumination.

**SECTION** Energy Conversion and Storage



Organic solar cells utilize a donor–acceptor system to break up excitons into free carriers.<sup>1</sup> In the bulk heterojunction (BHJ) structure, these donor–acceptor materials are intimately mixed to ensure that all generated excitons reach an interface before recombining.<sup>2</sup> Energy disorder in the materials, represented by the distribution of the electronic density of states (DOS) of donor and acceptor materials forming the active layer, plays a fundamental role in governing the physical processes in these devices and their limitations for solar energy conversion. A key factor to be improved in organic solar cells is recombination between electrons in the acceptor lowest unoccupied molecular orbital (LUMO) and holes in the donor highest occupied molecular orbital (HOMO). The open-circuit voltage  $V_{oc}$  is found to scale with the difference between the HOMO of the donor and the LUMO of the acceptor materials,<sup>3–5</sup> suggesting that recombination losses mainly take place at the donor/acceptor interface.<sup>6–9</sup> However, the donor HOMO and acceptor LUMO levels are usually determined from cyclic voltammetry of the respective materials in solution, sometimes in combination with absorption experiments.<sup>10</sup> A detailed knowledge of the relevant electronic state distributions for the materials after forming the blend, in connection with device operation parameters, is required to improve device quality, and this is the topic of this Letter.

We have recently reported capacitance and carrier lifetime measurements extracted from impedance spectroscopy measurements combined with steady-state illumination to derive recombination kinetics and DOS population in BHJ solar cells.<sup>11</sup> It was found that electronic states in the fullerene display broad energy dispersion. The shape of the DOS has the Gaussian form, as generally expected in organic materials affected by chemical or structural defects,<sup>12,13</sup> but the higher lying energy states in the fullerene are not accessible because the recombination kinetics severely limits the occupation to the DOS tail. In general, the presence of energy disorder in the materials forming the solar cell is found to cause a decisive influence in the mechanisms determining the photovoltaic properties. In organic blends with phase segregation on the nanometer scale, disorder eliminates any coherence effects, and all carriers will be completely localized. As an introduction to the interpretation of our experimental results, we discuss some effects of carrier localization at the energy disordered landscape, using the scheme of Figure 1, that is based on recent reports of BHJ solar cells.<sup>11,14</sup>

**Received Date:** July 14, 2010

**Accepted Date:** August 6, 2010

**Published on Web Date:** August 12, 2010

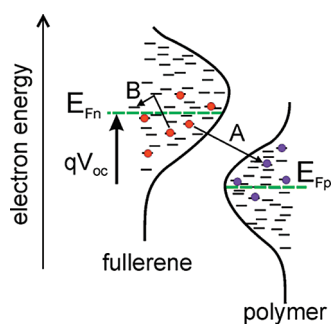


**Figure 1.** Pictorial energy scheme suggesting the Gaussian density of states (DOS) in both the polymer and fullerene materials forming a bulk heterojunction solar cell and some electronic properties determining the cell performance. Thermalized electrons in the fullerene and thermalized holes in the polymer are located predominantly, respectively, in the lower and upper tails of the DOS. The distribution of charges determines the Fermi levels of electrons ( $E_{Fn}$ ) and holes ( $E_{Fp}$ ), which difference gives the open-circuit voltage  $V_{OC}$  ( $q$  is the elementary charge). Recombination of an electron in a localized state in the fullerene with a hole in the polymer is indicated by an arrow (A). An electron can also be separated from the interface by hopping events to nearby available localized states (B).

The first important aspect is that accumulation of photo-generated electrons and holes in localized states sets the Fermi levels for electrons ( $E_{Fn}$ ) and holes ( $E_{Fp}$ ) in the fullerene and in the polymer, respectively. Therefore, the DOS determines a relationship between carrier density and voltage in the cell, as expressed quantitatively in eq 3, below, which is distinctively different from the standard expressions for electrons statistics in crystalline semiconductors. This relationship places constraints on the  $V_{OC}$  values. For example, comparing two fullerene materials with higher and lower number density of states (and the same properties of LUMO level, recombination rate, etc.), the first one will produce a higher photovoltage in a BHJ because the  $E_{Fn}$  will rise higher for a given number of carriers received. This is the specific point we discuss in this Letter, by a comparison of BHJ solar cells consisting of a poly(3-hexylthiophene) (P3HT) donor and two fullerene acceptors, either [6,6]-phenyl- $C_{61}$ -butyric acid methyl ester (PCBM) or 4,4'-dihexyloxydiphenylmethano[60]fullerene (DPM<sub>6</sub>). (See Figure 2.)

In addition to the purely thermodynamic aspects, that is, the charging of the DOS, the energy disorder also has a strong influence on a series of kinetics aspects that control the performance of the solar cell.<sup>15</sup> In effect, the distribution of localized states determines to an important extent the charge transfer events for electron transfer in exciton dissociation, the motion of electron escape by hopping (process B in Figure 1), and perhaps most important of all, the rates of recombination of electrons and holes. Given a certain rate of photogeneration, the number of carrier at steady state is set by the recombination rate. Which is the mechanism of recombination? Because the measurements show that carriers are immobilized at localized states, it is likely that recombination occurs from an electron in a localized state meeting a hole also in a localized state in the polymer, as suggested by an arrow in Figure 1 (process A).<sup>11,14</sup> In consequence, the disorder may determine the rate of exciton dissociation at the interface,<sup>16</sup> the probability

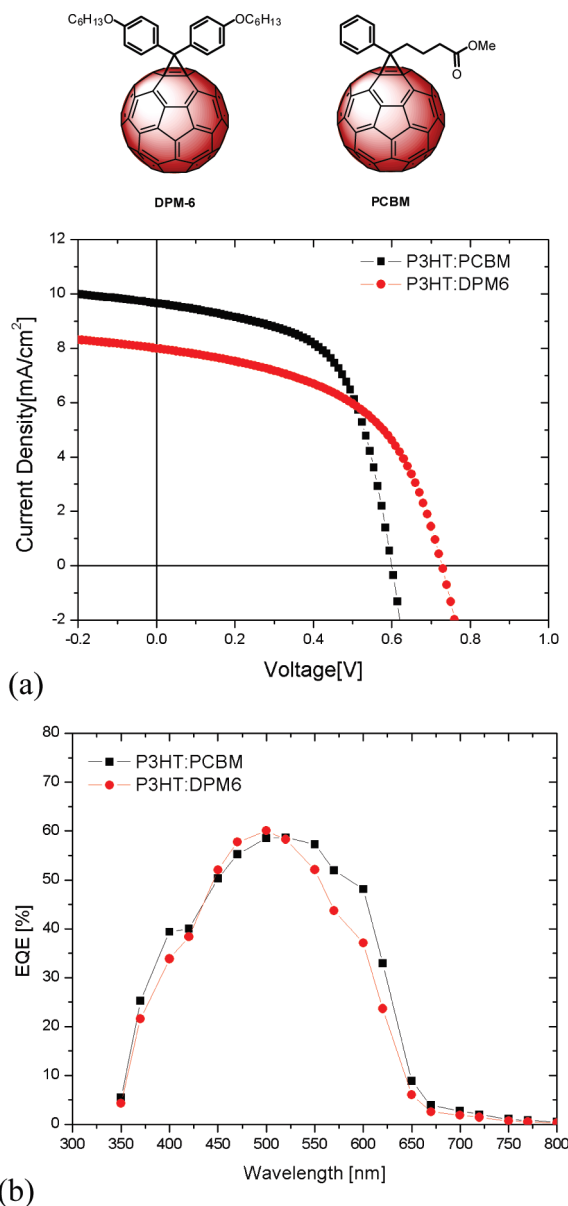


**Figure 2.** (a) Current density ( $j$ ) versus voltage ( $V$ ) characteristics for a P3HT/PCBM (black squares) and P3HT/DPM<sub>6</sub> (red circles) solar cells and fullerene chemical structure. (b) External quantum efficiency for typical P3HT/PCBM (black squares) and P3HT/DPM<sub>6</sub> (red circles) solar cells.

of escape of an electron at the interface from a geminate hole, the mobility of electrons across the fullerene network, and so on.

The electron acceptor materials used in this study, PCBM and DPM<sub>6</sub>, show the following properties.<sup>17</sup> The different functionalization of the fullerene cage leads to a similar LUMO level, as determined from cyclic voltammetry, and pure fullerene films show relatively similar charge transport capabilities. This in turn leads to a similar optimal donor/acceptor weight ratio of 1:1 of the active layer. Differences in film morphology have been observed, however, with DPM<sub>6</sub> showing a reduced tendency to crystallize and phase separate from the P3HT.

**Table 1.** Solar Cell Parameters under 1 Sun Irradiation Conditions Extracted from  $j$ - $V$  Curve and Impedance Measurements

fullerene	$j_{sc}$ (mA cm <sup>-2</sup> )	$V_{OC}$ (V)	$FF$	$\eta$ (%)	$n$ (cm <sup>-3</sup> )	$\tau$ ( $\mu$ s)
PCBM	9.94	0.600	0.52	3.10	$4.0 \times 10^{16}$	6.0
DPM <sub>6</sub>	7.52	0.728	0.51	2.60	$3.5 \times 10^{15}$	3.8

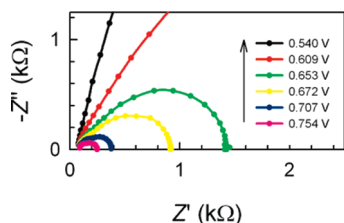


**Figure 3.** Impedance spectra measured under different irradiation intensities (open-circuit conditions) for DPM<sub>6</sub>-based devices.  $V_{OC}$  is indicated. The low-frequency response is modeled by means of a parallel RC subcircuit.

The BHJ solar cell devices made from PCBM and DPM<sub>6</sub> blends with P3HT show differences of performance.<sup>17</sup> (See Table 1 and Figure 2a.) A significant shift of 0.125 V in the output open-circuit photovoltage is registered under standard AM1.5G conditions (1000 W m<sup>-2</sup> of integrated power density). Such a large shift in open circuit voltage has been observed only for fullerenes with a significantly higher reduction potential.<sup>18–21</sup> DPM<sub>6</sub> shows lower short circuit current due to a reduced shoulder in the red part of the external quantum efficiency (EQE). (See Figure 2b.) Similar power conversion efficiencies for both acceptors were registered due to partial compensation of the difference in voltages and currents. As previously anticipated, we show in this work that the shift in the  $V_{OC}$  is caused by the different occupancy of the DOS of both fullerenes. Whereas DPM<sub>6</sub> exhibits a full occupation of the electronic band, the electronic occupancy is restricted to the tail of the DOS in the case of PCBM-based devices.

Impedance measurements were performed under open-circuit conditions in such a way that the applied bias voltage compensates the effect of the photovoltage ( $j_{dc} = 0$ ); that is, photocurrent is canceled by the recombination flow,  $j_{gen} = j_{rec}$ . Details of the impedance measuring conditions are provided elsewhere.<sup>11</sup> The impedance spectra of DPM<sub>6</sub>-based solar cells at different illumination intensities are shown in Figure 3. Similar impedance responses in the low-frequency region were observed for PCBM-based devices.<sup>11</sup> As observed in Figure 3, the spectra are characterized by a major RC arc. Such low-frequency arc is interpreted in terms of the chemical capacitance and recombination resistance<sup>22</sup> and provides the essential information on carrier accumulation and recombination at each measurement potential.

Essential to the interpretation adopted in this Letter for open-circuit voltage is the interpretation of the capacitance measured by IS. We have already reported the properties of the capacitance in BHJ solar cells.<sup>11,23,24</sup> In brief, we find the following behavior: (a) At deep reverse, the organic blend is fully depleted of carriers, and the dielectric (geometric) capacitance of the blend is measured. (b) At reverse and zero bias, an interfacial capacitance is observed, related to a

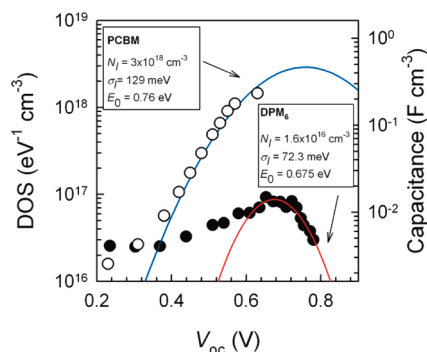


**Figure 4.** Capacitance values extracted from fits of the low-frequency arc of the impedance spectra as a function of  $V_{OC}$  reached under varying illumination levels. White dots correspond to PCBM-based solar cells and black dots to DPM<sub>6</sub>-based solar cells. Gaussian DOS (solid lines) and distribution parameters resulting from fits.

Schottky barrier at the cathode, which consists of depletion of the majority p-carriers.<sup>24</sup> (c) At further forward bias, a chemical capacitance is observed, in common with other types of solar cells such as crystalline silicon<sup>25</sup> or dye-sensitized solar cells.<sup>22</sup> (d) At further forward bias, the capacitance decreases because of a negative contribution.<sup>24,26</sup>

Of interest here is the capacitance measured under open-circuit conditions related to the ability of the solar cell to store charge under influence of illumination; hereafter, we focus on this contribution. In contrast with the standard dielectric capacitor, this capacitance is denoted as chemical because it describes a change in the electronic density that appears as a consequence of the displacement of the electrochemical potential (the Fermi level).<sup>27,28</sup> Assuming that the carriers follow the zero-temperature Fermi distribution, it can be shown that the chemical capacitance is proportional to the DOS,  $g(E)$ , at a given position of the Fermi level<sup>29</sup>

$$C_{\mu} = q^2 g(E_{Fn}) \quad (1)$$

As previously mentioned, the DOS in disordered organic conductors usually exhibits a Gaussian distribution.<sup>12</sup> Therefore, we have the expression

$$g(E) = \frac{N}{\sqrt{2\pi}\sigma} \exp\left[-\frac{(E-E_0)^2}{2\sigma^2}\right] \quad (2)$$

Here  $N$  accounts for the total DOS with mean energy  $E_0$  and width  $\sigma$ . The distribution of the DOS is broad if  $\sigma > k_B T$ . It should be noticed that the approximation in eq 1 strictly holds in the case of high (>1 %) occupancy levels.

By measuring the open-circuit capacitance, we have previously identified<sup>11</sup> an approximate Gaussian DOS associated with the LUMO manifold of the acceptor compound PCBM. Such an electronic band exhibits an electron density on the order of  $N_1 \approx (1 \text{ to } 3) \times 10^{18} \text{ cm}^{-3}$ . (See Figure 4.) This value appears to be very low in comparison with that derived from simple geometric considerations about the volume occupation of PCBM phase (van der Waals diameter of the PCBM molecule about 1 nm) because the expected total density

would be around  $N_{\text{PCBM}} = 10^{21} \text{ cm}^{-3}$ . The ratio  $N_i/N_{\text{PCBM}}$  remains within the range 0.1 to 0.2% for different cells. The Gaussian DOS resulting from the fits of several cells are centered at  $E_0 = 0.75$  to  $0.80 \text{ eV}$ , and the disorder parameter  $\sigma_1$  lies within the range 125–140 meV, consistent with the results of the decay of photogenerated carriers monitored by transient microwave conductivity measurements.<sup>30</sup> We conclude that the electronic levels monitored by the trail of the Fermi level as the voltage is increased can be associated with an intermediate band (IDOS) that is located below the upper lying LUMO manifold. These results suggest the existence of additional states at higher energies  $\sim 1.1 \text{ eV}$  corresponding to the fullerene LUMO DOS.

Chemical capacitance measurements on DPM<sub>6</sub>-based devices show a different result. A full electronic band is found by the capacitance measured at high open-circuit photovoltages, which slightly exceeds the geometrical capacitance value of  $\sim 30 \text{ nF cm}^{-2}$ . (See Figure 4.) This capacitance peak signals the presence of an intermediate band that is half-occupied at  $V_{\text{OC}} \approx 0.68 \text{ V}$ , again below the DPM<sub>6</sub> LUMO position at  $\sim 1.1 \text{ eV}$ . Values for  $N_i = (1 \text{ to } 2) \times 10^{16} \text{ cm}^{-3}$  were encountered, much smaller than the expected value for  $N_{\text{DPM}_6} = 10^{21} \text{ cm}^{-3}$ , in a similar fashion as that observed in the case of PCBM-based solar cells. This IDOS is found to be centered at  $E_0 = 0.675 \text{ eV}$ , and the disorder parameter  $\sigma_1$  results around 72 meV. The most significant feature in comparing the IDOS identified for PCBM and DPM<sub>6</sub> fullerenes is a difference of two orders of magnitude between the total number of electronic levels. It is around  $10^{16} \text{ cm}^{-3}$  for DPM<sub>6</sub>, whereas a density of  $10^{18} \text{ cm}^{-3}$  is exceeded in the case of PCBM.

It should be noted here that the measured capacitances on the order of 0.1 to  $1 \mu\text{F cm}^{-2}$  are hardly related to interfacial mechanisms. If one assumes eq 1 to be governing the occupation of interfacial states, the corresponding surface charge density would be within the orders  $10^{18}$ – $10^{20} \text{ cm}^{-2}$ , which has no physical meaning. As previously mentioned, an interfacial capacitance (due to a depletion layer at the cathode) is measured in another domain of bias potential (the initial rise in Figure 4) and can be characterized by Mott–Schottky behavior.

Recalling now the difference in the achieved open-circuit photovoltage between cells based on these two fullerenes (Table 1 and Figure 4), one can estimate the amount of photogenerated charges under 1 sun irradiation conditions. Such a photogenerated charge is approximated by the area below the DOS curve in Figure 4 as

$$n = \frac{1}{q} \int_0^{V_{\text{OC}}} C_{\mu}(V) dV \quad (3)$$

By applying eq 3, one can determine the density of photogenerated charges that result in  $n_{\text{PCBM}}(V_{\text{OC}} = 0.60 \text{ V}) = 4 \times 10^{16} \text{ cm}^{-3}$  and  $n_{\text{DPM}_6}(V_{\text{OC}} = 0.73 \text{ V}) = 3.5 \times 10^{15} \text{ cm}^{-3}$ . Despite DPM<sub>6</sub> exhibiting an intermediate band (Figure 4) that becomes fully occupied at high irradiance levels, PCBM-based devices are able to accumulate more charge at lower-lying states because of the larger DOS. The difference of one order of magnitude in the amount of photogenerated charges

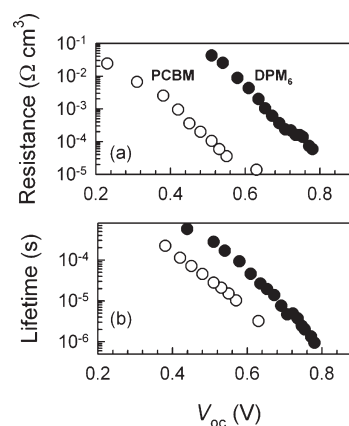


**Figure 5.** (a) Specific recombination resistance as a function of  $V_{\text{OC}}$  resulting from the analysis of low-frequency impedance under varying illumination levels. (b) Recombination time (effective lifetime) as a function of  $V_{\text{OC}}$  calculated from the  $RC$  time constant.

cannot be solely explained by considering the difference in short-circuit current. (See Table 1.) For DPM<sub>6</sub>-based devices,  $j_{\text{SC}}$  is reduced by only 25% with respect to PCBM-based devices. Hence the PCBM cell's ability to accumulate photogenerated charges should also be related to a reduced recombination rate. Because solar cells under open-circuit conditions operate under kinetic balance between photogeneration ( $G$ ) and recombination rates ( $U$ ), that is,  $G = U$ ,<sup>31</sup> and taking into account the fact that  $U \approx n/\tau$  (where  $\tau$  is the recombination time), it follows that  $\tau_{\text{DPM}_6} < \tau_{\text{PCBM}}$  under 1 sun irradiation conditions. We will next explore in more detail the validity of this argument by extracting the recombination resistance and lifetime from the impedance measurements.

As mentioned above the low frequency arc is attributed to charge recombination in the photoactive blend. The resistance of the arc is the differential recombination resistance  $R_{\text{rec}}$  (per unit volume), which is related to the recombination current density  $j_{\text{rec}}$  as<sup>22</sup>

$$R_{\text{rec}} = L \left( \frac{dj_{\text{rec}}}{dV} \right)^{-1} \quad (4)$$

with  $L$  being the absorbing layer thickness. We observe in Figure 5a a nearly exponential decrease in the recombination resistance with increasing voltage  $R_{\text{rec}} \propto \exp(-\beta V_{\text{OC}}/k_{\text{B}}T)$ , where  $\beta \approx 0.70$  to  $0.76$ . Remarkably, there is a shift in the recombination resistance with respect to  $V_{\text{OC}}$ , which approximately coincides with the photovoltage difference between the two devices. The recombination time (lifetime) can be calculated from the impedance response time as  $\tau = R_{\text{rec}}C_{\mu}$ , and it is plotted in Figure 5b as a function of  $V_{\text{OC}}$ . We can extract recombination time values under 1 sun irradiation conditions, which results in  $\tau_{\text{PCBM}}(V_{\text{OC}} = 0.60 \text{ V}) = 6.0 \mu\text{s}$ , whereas  $\tau_{\text{DPM}_6}(V_{\text{OC}} = 0.73 \text{ V}) = 3.8 \mu\text{s}$ . As expected from simple arguments on the recombination kinetics, we then observe that  $\tau_{\text{DPM}_6} < \tau_{\text{PCBM}}$ , with  $\tau_{\text{DPM}_6}$  being 40% smaller than  $\tau_{\text{PCBM}}$ .

The main conclusion of this work is that the output  $V_{\text{OC}}$  reached by different fullerene acceptor materials in BHJ solar

cells is closely related to the amount and energy distribution of available electronic sites. Electronic carriers thermalize to lower-lying available levels under steady-state conditions of continuous irradiation and form a Gaussian distribution that sets the position of the Fermi level.<sup>11,14</sup> Thereby, we have observed that DPM<sub>6</sub>-based solar cells reach higher  $V_{OC}$  values because of a smaller IDOS that lies below the upper LUMO manifold of the fullerene. Remarkably, the existence of larger IDOS in the case of PCBM has the detrimental consequence of keeping the Fermi level within the tail of the distribution, therefore limiting the rise of the output  $V_{OC}$ . Because the main difference between PCBM and DPM<sub>6</sub> is observed to be the less crystalline nature of the latter, we suggest that the origin of the electronic intermediate bands lies in the existence of pure fullerene (PCBM) crystals with reduced energy gaps. Indeed, experiments changing the crystallinity of the donor material have shown a similar relationship between active layer crystallinity and open circuit voltage.<sup>32</sup>

The results discussed in this Letter underline the importance of the distribution of electronic states of the actual solid-state active layer. Whereas the HOMO and LUMO levels deduced from CV measurements give a first order approximation, it is the perturbation of these levels that governs the open circuit voltage in real devices. Recent results on the use of fullerene bisadducts have also shown a much larger increase in open circuit voltage versus PCBM when taking into account only the change of their LUMO levels.<sup>18,21</sup> Similar to the work presented here, the origin of this behavior is likely to be a much more featured shape of the DOS, in this case caused by the existence of a multitude of isomers of the acceptor. Electrical measurements indeed show signs of IDOS states causing charge trapping in these devices.<sup>19</sup> The measurement technique presented here allows for a direct insight into the size and shape of these energy states.

In summary, it is derived from this study that a determining factor of both open-circuit voltages is the amount and energy distribution of intermediate electronic states (IDOS) below the LUMO level of the acceptor molecules. Less crystalline fullerenes (DPM<sub>6</sub>) allow for a higher rise of the Fermi level by a reduction of the available number of electronic states.

## AUTHOR INFORMATION

### Corresponding Author:

\*To whom correspondence should be addressed. (G.G.-B.) E-mail: garciag@fca.uji.es. Tel.: +34 964387548. (J.B.) E-mail: bisquert@fca.uji.es. Tel.: +34 964387541.

**ACKNOWLEDGMENT** This work has been supported by the Spanish Ministry of Science and Innovation (MICINN) under projects PS-120000-2007-1 (FOTOMOL) 2008, MAT2006-28185-E, MAT2007-61584, Consolider Ingenio HOPE CSD2007-00007 and CSD2007-00010. N.M. acknowledges projects CTQ2008-00795/BQU, MADRISOLAR-2 S2009/PPQ-1533, and J.B. the Generalitat Valenciana project PROMETEO/2009/058. We especially thank Alejandra Soriano for the careful device preparation.

## REFERENCES

- (1) Tang, C. W. Two-Layer Organic Photovoltaic Cell. *Appl. Phys. Lett.* **1986**, *48*, 183–185.
- (2) Yu, G.; Gao, J.; Hummelen, J. C.; Wudl, F.; Heeger, A. J. Polymer Photovoltaic Cells: Enhanced Efficiencies via a Network of Internal Donor–Acceptor Heterojunctions. *Science* **1995**, *270*, 1789–1791.
- (3) Gadisa, A.; Svensson, M.; Andersson, M. R.; Inganäs, O. Correlation Between Oxidation Potential and Open-Circuit Voltage of Composite Solar Cells on Blends of Polythiophenes/Fullerene Derivative. *Appl. Phys. Lett.* **2004**, *84*, 1609–1611.
- (4) Scharber, M.; Mühlbacher, D.; Koppe, M.; Denk, P.; Waldauf, C.; Heeger, A. J.; Brabec, C. J. Design Rules for Donor Bulk-Heterojunction Solar Cells-Towards 10% Energy-Conversion Efficiency. *Adv. Mater.* **2006**, *18*, 789–794.
- (5) Veldman, D.; Meskers, S. C. J.; Janssen, R. A. J. The Energy of Charge-Transfer States in Electron Donor–Acceptor Blends: Insights into the Energy Losses in Organic Solar Cells. *Adv. Funct. Mater.* **2009**, *19*, 1939–1948.
- (6) Lemaur, V.; Steel, M.; Beljonne, D.; Brédas, J. L.; Cornil, J. Photoinduced Charge Generation and Recombination Dynamics in Model Donor/Acceptor Pairs for Organic Solar Cells Applications: A Full Quantum-Chemical Treatment. *J. Am. Chem. Soc.* **2006**, *127*, 6077–6086.
- (7) Rand, B. P.; Burk, D. P.; Forrest, S. R. Offset Energies at Organic Semiconductor Heterojunctions and Their Influence on the Open-Circuit Voltage of Thin-Film Solar Cells. *Phys. Rev. B* **2007**, *75*, 115327.
- (8) Vandewal, K.; Gadisa, A.; Oosterbaan, W. D.; Bertho, S.; Banishoeib, F.; Severen, I. V.; Lutsen, L.; Cleij, T. J.; Vanderzande, D.; Manca, J. V. The Relation Between Open-Circuit Voltage and the Onset of the Photocurrent Generation by Charge-Transfer Absorption in Polymer:Fullerene Bulk Heterojunction Solar Cells. *Adv. Funct. Mater.* **2008**, *18*, 2064–2070.
- (9) Tvingstedt, K.; Vandewal, K.; Gadisa, A.; Zhang, F.; Manca, J.; Inganäs, O. Electroluminescence from Charge Transfer States in Polymer Solar Cells. *J. Am. Chem. Soc.* **2009**, *131*, 11819–11824.
- (10) Kirchartz, T.; Taretto, K.; Rau, U. Efficiency Limits of Organic Bulk Heterojunction Solar Cells. *J. Phys. Chem. C* **2009**, *113*, 17958–17966.
- (11) Garcia-Belmonte, G.; Boix, P. P.; Bisquert, J.; Sessolo, M.; Bolink, H. J. Simultaneous Determination of Carrier Lifetime and Electron Density-Of-States in P3HT:PCBM Organic Solar Cells Under Illumination by Impedance Spectroscopy. *Sol. Energy Mater. Sol. Cells* **2010**, *94*, 366–375.
- (12) Bäessler, H. Charge Transport in Disordered Organic Photoconductors. *Phys. Status Solidi B* **1993**, *175*, 15–56.
- (13) Kaake, L. G.; Barbara, P. F.; Zhu, X.-Y. Intrinsic Charge Trapping in Organic and Polymeric Semiconductors: A Physical Chemistry Perspective. *J. Phys. Chem. Lett.* **2010**, *1*, 628–635.
- (14) Garcia-Belmonte, G.; Bisquert, J. Open-Circuit Voltage Limit Caused by Recombination Through Tail States in Bulk Heterojunction Polymer-Fullerene Solar Cells. *Appl. Phys. Lett.* **2010**, *96*, 113301.
- (15) Clarke, T. M.; Durrant, J. R. Charge Photogeneration in Organic Solar Cells. *Chem. Rev.*, published online Jan 11, <http://dx.doi.org/10.1021/cr900271s>.
- (16) Barth, S.; Hertel, D.; Tak, Y.-H.; Bäessler, H.; Hörhold, H. H. Geminate Pair Dissociation in Random Organic Systems. *Chem. Phys. Lett.* **1997**, *274*, 165–170.
- (17) Bolink, H. J.; Coronado, E.; Forment-Aliaga, A.; Lenes, M.; La Rosa, A.; Filippone, S.; Martin, N. Polymer Solar Cells Based on Diphenylmethanofullerenes with Reduced Sidechain Length. *J. Mater. Chem.* **2010**, DOI: 10.1039/c0jm01160f.
- (18) Lenes, M.; Wetzelaer, G. A. H.; Kooistra, F. B.; Veenstra, S. C.; Hummelen, J. C.; Blom, P. W. M. Fullerene Bisadducts for

- Enhanced Open-Circuit Voltages and Efficiencies in Polymer Solar Cells. *Adv. Mater.* **2008**, *20*, 2116–2119.
- (19) Lenes, M.; Shelton, S. W.; Sieval, A. B.; Kronholm, D. F.; Hummelen, J. C.; Blom, P. W. M. Electron Trapping in Higher Adduct Fullerene-Based Solar Cells. *Adv. Funct. Mater.* **2009**, *19*, 3002–3007.
- (20) Ross, R. B.; Cardona, C. M.; Guldi, D. M.; Sankaranarayanan, S. G.; Reese, M. O.; Kopidakis, N.; Peet, J.; Walker, B.; Bazan, G. C.; Van Keuren, E.; et al. Endohedral Fullerenes for Organic Photovoltaic Devices. *Nat. Mater.* **2009**, *8*, 208–212.
- (21) He, Y.; Chen, H.-Y.; Hou, J.; Li, Y. Indene-C60 Bisadduct: A New Acceptor for High-Performance Polymer Solar Cells. *J. Am. Chem. Soc.* **2010**, *132*, 1377–1382.
- (22) Bisquert, J.; Fabregat-Santiago, F.; Mora-Seró, I.; Garcia-Belmonte, G.; Giménez, S. Electron Lifetime in Dye-Sensitized Solar Cells: Theory and Interpretation of Measurements. *J. Phys. Chem. C* **2009**, *113*, 17278–17290.
- (23) Bisquert, J.; Garcia-Belmonte, G.; Munar, A.; Sessolo, M.; Soriano, A.; Bolink, H. J. Band Unpinning and Photovoltaic Model for P3HT:PCBM Organic Bulk Heterojunctions Under Illumination. *Chem. Phys. Lett.* **2008**, *465*, 57–62.
- (24) Garcia-Belmonte, G.; Munar, A.; Barea, E. M.; Bisquert, J.; Ugarte, I.; Pacios, R. Charge Carrier Mobility and Lifetime of Organic Bulk Heterojunctions Analyzed by Impedance Spectroscopy. *Org. Electron.* **2008**, *9*, 847–851.
- (25) Mora-Seró, I.; Garcia-Belmonte, G.; Boix, P. P.; Vázquez, M. A.; Bisquert, J. Impedance Characterisation of Highly Efficient Silicon Solar Cell under Different Light Illumination Intensities. *Energy Environ. Sci.* **2009**, *2*, 678–686.
- (26) Lungenschmied, C.; Ehrenfreund, E.; Sariciftci, N. S. Negative Capacitance and its Photo-Inhibition in Organic Bulk Heterojunction Devices. *Org. Electron.* **2009**, *10*, 115–118.
- (27) Bisquert, J. Chemical Capacitance of Nanostructured Semiconductors: Its Origin and Significance for Heterogeneous Solar Cells. *Phys. Chem. Chem. Phys.* **2003**, *5*, 5360–5364.
- (28) Bisquert, J.; Fabregat-Santiago, F.; Mora-Seró, I.; Garcia-Belmonte, G.; Barea, E. M.; Palomares, E. A Review of Recent Results on Electrochemical Determination of the Density of Electronic States of Nanostructured Metal-Oxide Semiconductors and Organic Hole Conductors. *Inorg. Chim. Acta* **2008**, *361*, 684–698.
- (29) Bisquert, J.; Garcia-Belmonte, G.; García-Cañadas, J. Effect of the Gaussian Energy Dispersion on the Statistics of Polarons and Bipolarons in Conducting Polymers. *J. Chem. Phys.* **2004**, *120*, 6726–6733.
- (30) Moehl, T.; Kytin, V. G.; Bisquert, J.; Kunst, M.; Bolink, H. J.; Garcia-Belmonte, G. Relaxation of Photogenerated Carriers in P3HT:PCBM Organic Blends. *ChemSusChem* **2009**, *2*, 314–320.
- (31) Kawatsu, T.; Coropceanu, V.; Ye, A.; Brédas, J. L. Quantum-Chemical Approach to Electronic Coupling: Application to Charge Separation and Charge Recombination Pathways in a Model Molecular Donor–Acceptor System for Organic Solar Cells. *J. Phys. Chem. C* **2008**, *112*, 3429–3433.
- (32) Vandewal, K.; Oosterbaan, W. D.; Bertho, S.; Vrindts, V.; Gadisa, A.; Lutsen, L.; Vanderzande, D.; Manca, J. V. Varying Polymer Crystallinity in Nanofiber Poly(3-Alkylthiophene): PCBM Solar Cells: Influence on Charge-Transfer State Energy and Open-Circuit Voltage. *Appl. Phys. Lett.* **2009**, *95*, 123303.